



INFLUENCE OF BLADE NUMBER ON AERODYNAMIC NOISE OF PROPELLER FANS FOR OUTDOOR UNIT OF AIR-CONDITIONER

Taku IWASE¹, Tetsushi KISHITANI², Masato FURUKAWA³

¹ *Hitachi, Ltd., Hitachi Research Laboratory, 832-2, Horiguchi, Hitachinaka, Ibaraki, Japan*

² *Hitachi Appliances, Inc., 390, Muramatsu, Shimizu, Shizuoka, Japan*

³ *Kyushu University, 744, Motooka, Nishi-ku, Fukuoka, Japan*

SUMMARY

Flow fields in 2-blade and 4-blade half-ducted propeller fans for the outdoor units of air-conditioners were calculated with finite element method-based large eddy simulation with the aim of investigating what influence of blade number had on aerodynamic noise in this study. As a result, we confirmed that the tip vortex and leading edge separation vortex had a great influence on half-ducted propeller fans. The tip vortex trajectory and the blade pitch of the 2-blade propeller fan were longer than those of the 4-blade propeller fan. These suppressed the interaction between the tip vortex, the ring, and the adjacent blade. The 2-blade propeller fan was therefore more silent than the 4-blade propeller fan.

INTRODUCTION

Development of silent air-conditioners is one of the most important problems in recent changes to life-styles because aerodynamic noise from fans contributes to a large percentage of the overall noise from air-conditioners. Therefore, the development of silent fans would contribute to reducing the noise levels of air-conditioners. The fans in many air-conditioners with outdoor units have a short casing that only covers the near region of the propeller tips, which has been designed for compactness. As a result, part of the blade tip near its leading edge is open to the upstream. These propeller fans are called half-ducted propeller fans. They have a very complicated flow field near the propeller tips.

Half-ducted propeller fans were mainly developed by using experimental methods. Predictions of aerodynamic noise were based on estimates from static flow field characteristics and experimental coefficients [1]. However, it is difficult to develop radically silent fans by using traditional methods. We therefore need new methods of predicting aerodynamic noise and developing silent fans.

Computational fluid dynamics (CFD) is a powerful tool for solving these needs. Many researchers have recently studied flow fields by using large eddy simulation (LES) [2, 3, 4, and 5].

Many researchers have also studied the development of silent fans. Beiler et al. analyzed blade-to-blade flow fields by using CFD and hot wire, and they developed a silent fan with skewed blades [6]. Okamoto et al. proposed an optimized blade shape for a propeller fan by using an inverse design method and CFD [7]. Sugio optimized blade number of propeller fan [8]. However, there were few studies about detail investigation between blade number and aerodynamic noise.

The final goal of our study was aimed at developing methods of predicting aerodynamic noise and designing silent fans. Investigations in the present study were therefore implemented with CFD to analyze what influence of blade number had on aerodynamic noise in half-ducted propeller fans.

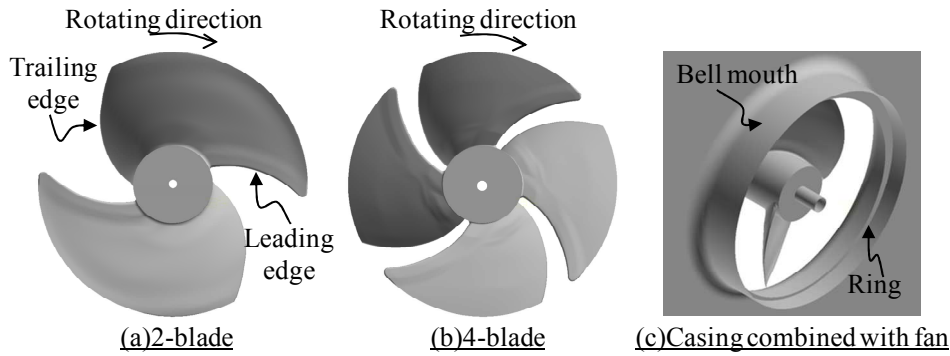


Figure 1: Configurations for intended fans

Table 1: Design specifications

	2-blade		4-blade	
	Hub	Tip	Hub	Tip
Radius ratio	0.29	1.00	0.29	1.00
Setting angle[deg]	35	24	35	27
Blade length[mm]	310	760	160	460

TEST PROPELLER FANS

The present study was carried out on the half-ducted propeller fans used in the outdoor units of air-conditioners. 2-blade and 4-blade propeller fans were intended to analyze what influence of blade number had on aerodynamic noise. Figure 1 shows configuration of the intended fans. The propeller tip diameter was 644 mm. Table 1 summarizes design specifications for the fans. A casing consists of a bell mouth and a ring inner side for the bell mouth. The ring only covers the rear region of the propeller tip. The noise level of the 2-blade propeller fan was smaller than that of the 4-blade propeller fan by 5.1 dB experimentally at an operating flow coefficient of $\phi=0.28$. The static pressure rise coefficients of both fans were $\psi_s=0.14$, which were almost the same as the operating flow coefficient. The flow coefficient and static pressure rise coefficient are defined as follows:

$$\phi = \frac{4Q}{\pi D_t^2 u_t} \quad (1)$$

$$\psi_s = \frac{2\Delta P_s}{\rho u_t^2} \quad (2)$$

Here Q is the volume flow rate, ΔP_s is the static pressure rise, and u_t is the propeller tip speed. The ρ is the density and D_t is the propeller tip diameter.

METHODS OF NUMERICAL SIMULATION

Large Eddy Simulation

The numerical simulation code employed throughout the LES was called FrontFlow/blue (FFB), which was developed by Kato et al. and successfully used for several applications [2, 3, 4]. The code was based on the finite element discretization of filtered incompressible continuity and Navier Stokes equations. The Dynamic Smagorinsky model was used as a sub-grid scale model.

The interaction between the rotating propeller and the stationary parts was taken into account by dynamically oversetting the grids from multiple frames of reference [2]. Each grid part included appropriate margins of overlap with their neighboring grid parts downstream and upstream. The values for static pressure and velocity components in the margin were interpolated in corresponding neighboring elements for each time step.

Computational Conditions

Figure 2 shows computational model. Table 2 lists the number of grid elements. The computational model consists of three parts, i.e., the inlet, propeller, and outlet parts. The propeller part is in the rotating frame of reference. The inlet and the outlet parts are in the stationary frames. The grid is composed of hexahedral elements. An additional pipe was added to the end of the box for the outlet part to stabilize calculations. The number of grid elements per blade pitch was approximately 2.7 million. The grids were generated for capturing main flow structures, which played dominant roles with aerodynamic noise.

The calculated flow rate and rotational speed were 100 m³/min and 550 rpm (operating flow coefficient of $\phi=0.28$). The time increment was $1.33 \cdot 10^{-5}$ sec. This time increment corresponded to 8,192 time steps by using a single revolution of the propeller. FFB used in the present study can calculate stably when CFL (Courant-Friedrichs-Lewy Condition) was lower than 5. The time increment was therefore decided in the condition of $CFL < 5$. The calculated results were sampled during four revolutions of the propeller.

Methods Used for Evaluations

The trajectory of the vortex center was identified with a semi-analytic method, which was based on critical-point theory, to enable the complicated flow field in the propeller fans to be better understood. It was possible to visualize the vortex core according to this method. Normalized helicity was evaluated along the vortex cores to quantitatively analyze the nature of the vortex. The normalized helicity, H_n , is defined by the following equation.

$$H_n = \frac{\vec{\xi} \cdot \vec{w}}{\|\vec{\xi}\| \|\vec{w}\|} \quad (3)$$

Here ξ is the absolute vorticity and w is the relative velocity. The normalized helicity is defined from the cosine of the angle between absolute vorticity and relative velocity. If $H_n = \pm 1$, this indicates there is a vortex core for the longitudinal vortex in the region. The plus and minus signs of normalized helicity denote the direction of rotation of the vortex. Visualizations of the vortex core and normalized helicity are useful tools for investigating the flow field of turbo-machinery [5, 9].

Aerodynamic noise was calculated with Curle's equation [10] defined by the following Equation. The sound source was assumed to be acoustically compact.

$$\rho - \rho_0 = \frac{1}{4\pi c_0^3} \frac{x_i}{r^2} \frac{\partial}{\partial t} \int_S n_i p dS \quad (4)$$

Here, ρ is the instant density, ρ_0 is the density in a uniform medium at rest, and c_0 is the sound speed. x_i is the observation point, r is the distance between the observation point and the sound source, and n_i is the outward normal vector on solid surface S . p represents static pressure fluctuations on solid surface S .

Ffowcs Williams-Hawkings (FWH) equation is well suited for predicting aerodynamic noise in the case of rotating surface. However, we used equation (4) aimed at verification of sound source magnitude relation in the present study. On the other hand, FFB can calculate the sound pressure spectrums by equation (4) from the calculated flow field results easily and speedily. We therefore used equation (4) by using this FFB's function as a first step of sound prediction.

Static pressure fluctuations p are related to velocity fluctuations near solid surface S . To investigate the relationship between the flow field and aerodynamic noise, turbulence intensity T_i , defined by the following equation, is therefore adopted as an indicator related to static pressure fluctuation on the blade and casing surfaces.

$$T_i = \sqrt{\frac{v_x'^2 + v_y'^2 + v_z'^2}{3u_t^2}} \quad (6)$$

Here, v_x' , v_y' , and v_z' are the three components of velocity fluctuations.

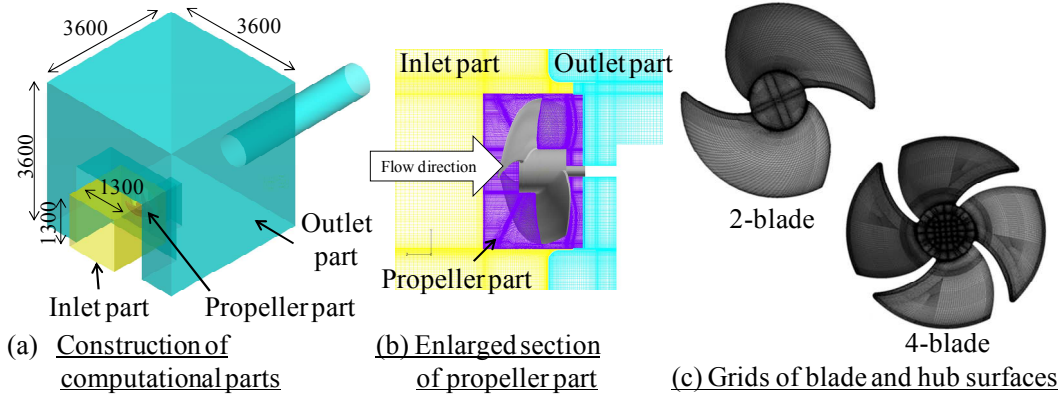


Figure 2: Computational model

Table 2: Number of grid elements

	Inlet part	Propeller part	Outlet part	Total	Blade-to-blade
2-blade	2,029,760	5,564,384	5,507,024	13,101,168	2,782,192
4-blade	1,875,424	10,618,752	5,507,024	18,001,200	2,654,688

EXPERIMENTAL APPARATUS AND PROCEDURES

Fan Performance Test

Fan performance was measured to verify the calculated results. Fan performances in the present study denoted the flow rate, static pressure rise, shaft power, and aerodynamic noise. Figure 3 shows a photograph of the experimental apparatus we used in the fan performance test. We used a

double chamber complied with JIS B 8330, Japanese Industrial Standards “Testing methods for turbo-fans” for measurement of the flow rate and the static pressure rise. The flow rate and the static pressure rise measurement accuracy were $\pm 0.5\%$ and $\pm 4\%$ respectively from specification of differential pressure transmitter in the operating flow coefficient. The shaft power measurement accuracy was $\pm 0.6\%$ from specification of torque meter in the operating flow coefficient.

The measurements were conducted in an anechoic chamber room at the Hitachi Research Laboratory. A microphone was placed 1 m away and at 45 deg from trailing edge in the 75% propeller tip diameter. A wind screen was used for preventing influence of wake. The sound pressure spectrum measurement accuracy was ± 0.2 dB from specification of microphone. A Hanning window function was applied to all measured data sets to perform a fast Fourier transform.

Measurements of Velocity Distributions Downstream of Blades

We measured time-averaged velocity distributions and velocity fluctuations downstream of the blades to verify the calculated results. Figure 3 also shows photographs of the experimental apparatus we used to measure the velocity distributions. The measured flow rate and rotational speed were $100 \text{ m}^3/\text{min}$ and 550 rpm (operating flow coefficient of $\phi=0.28$), which were the same as those for the calculations.

The time-averaged velocity distributions were measured with a 5-hole type pitot tube. The pitot tube was traversed along the radial direction. It was placed 140 mm in the 2-blade propeller fan and 105 mm in the 4-blade propeller fan downstream of the trailing edge of the blade. The pitot tube measurement accuracy was $\pm 13\%$ from specification of differential pressure transmitter.

The velocity fluctuations were measured with an I-type hotwire probe, which was traversed along the radial direction. The hotwire probe was placed 100 mm downstream of the trailing edge of the blade. The hotwire probe was calibrated previously with range of measurement velocity. Absolute velocities were measured. Before the measurement by the hotwire probe, we checked the flow direction of the absolute velocities by using tuft. When we measured by the hotwire probe, it was fixed the flow direction. The velocity fluctuations were evaluated by the root mean square.

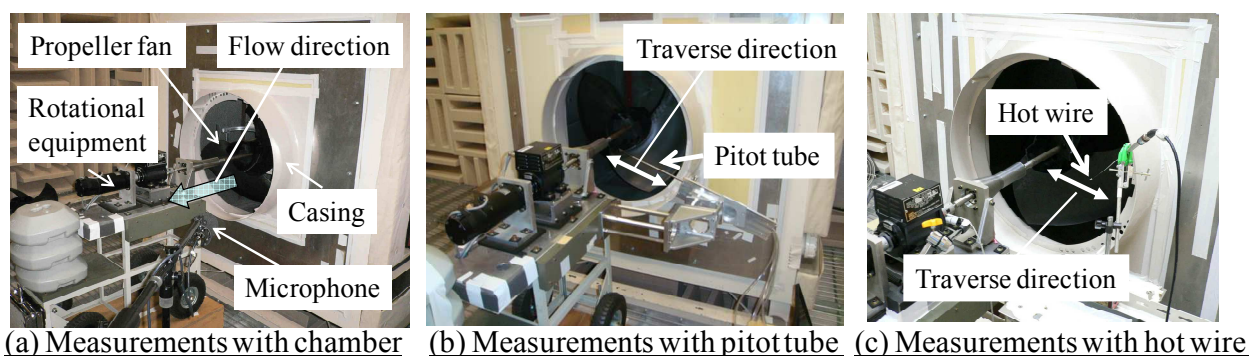


Figure 3: Photograph of experimental apparatus

RESULTS AND DISCUSSION

Validity of Numerical Simulations

First, we compared between calculated and experimental results for assessment of the LES quality. We actually compared fan performance, time-averaged velocity distributions, velocity fluctuations, and sound pressure spectrums.

Figure 4 compares the fan performance. The shaft power was normalized by the experimental shaft power of the 4-blade propeller fan at an operating flow coefficient of $\phi=0.28$. The calculated static

pressure of the 2-blade propeller fan was underestimated by 13% against the experimental results. The calculated shaft power of the 2-blade propeller fan was overestimated by 5% against the experimental results. The calculated static pressure and shaft power of the 4-blade propeller fan, on the other hand, were overestimated by 14%. The calculated and experimental shaft powers in the 2-blade propeller fan were smaller than those in the 4-blade propeller fan. The tendency between calculated and experimental results was therefore reasonably agreed.

Figure 5 compares the calculated and experimental time-averaged velocity distributions. The calculated absolute tangential velocity reasonably agreed with the experimental results. The qualitative tendency was captured between the calculated and the experimental results in the absolute radial velocity and absolute axial velocity. Yaw and pitch angles were within the range ± 30 degree, which were the calibrated ranges of pitot tube previously. The pitot tube was placed 140 mm in the 2-blade propeller fan and 105 mm in the 4-blade propeller fan downstream of trailing edge of the blade. We therefore could not confirm drastic change of flow direction by the tip vortex.

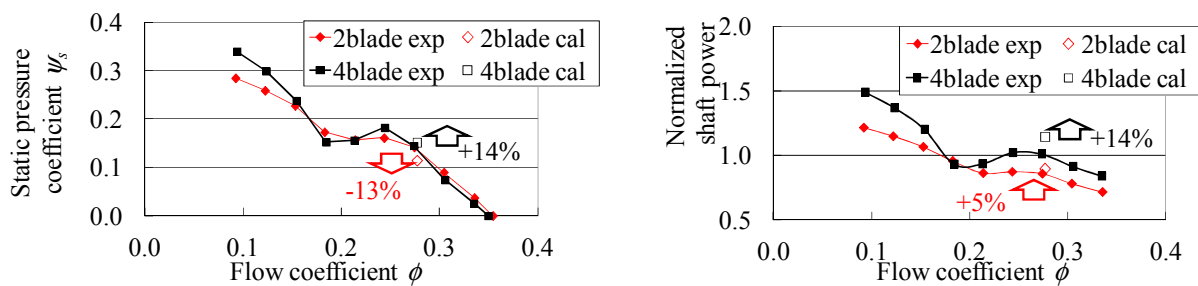


Figure 4: Comparison of fan performances

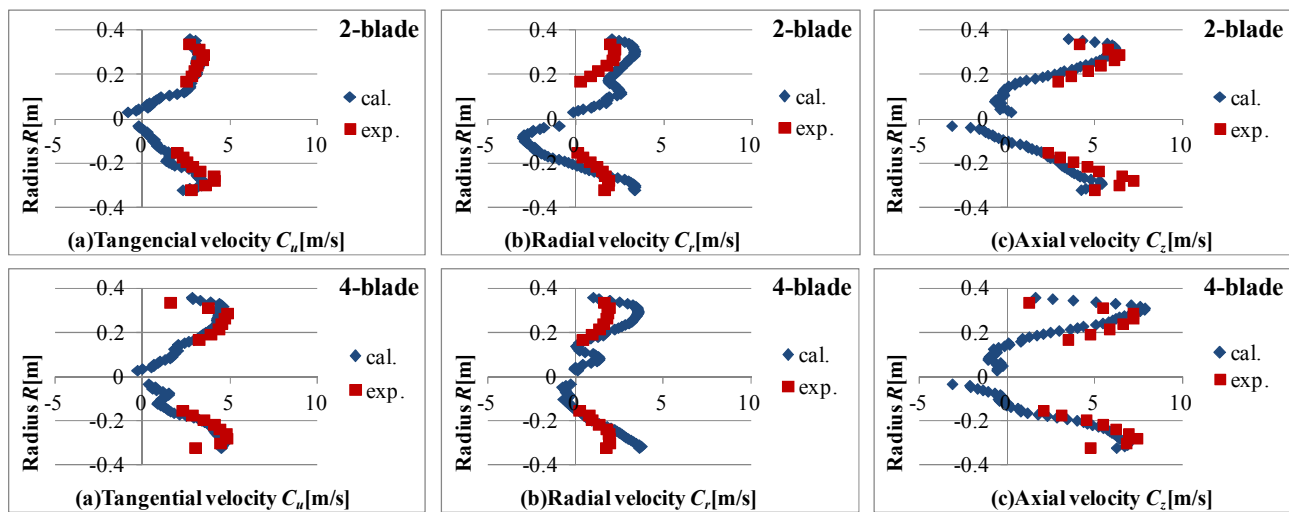


Figure 5: Comparison of calculated and experimental time-averaged velocity distributions

Figure 6 compares the calculated and experimental velocity fluctuations. A qualitative tendency was captured although the calculated results were overestimated against the experimental results. As mentioned in experimental apparatus chapter, we checked the flow direction of the absolute velocity by using tuft, before the measurement by hot wire probe. The hot wire probe was fixed the flow direction. We therefore think that the hotwire probe accuracy includes errors of calibration and fixing direction of the tuft.

Figure 7 compares the experimental absolute velocities between the pitot tube and the hotwire probe in order to investigate the hot wire measurement accuracy. The experimental results of the hot wire probe were overestimated by 31% in the case of small radius, and underestimated by 29% in the

case of large radius against those of the pitot tube. The experimental velocity fluctuations in Figure 6 therefore had possibilities that measurement accuracy was about $\pm 30\%$.

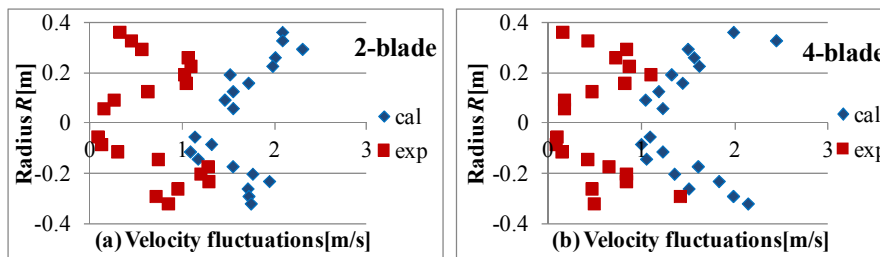


Figure 6: Comparison of calculated and experimental velocity fluctuations

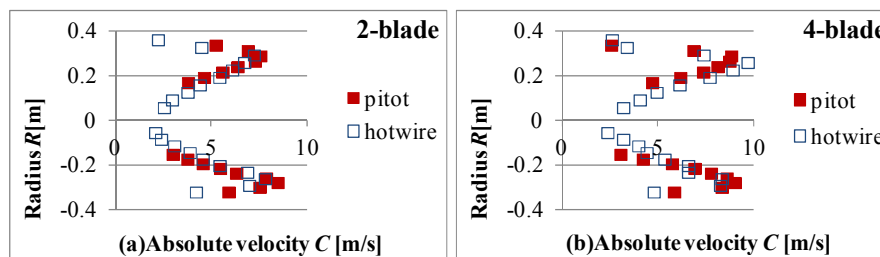


Figure 7: Comparison of calculated and experimental absolute velocities between pitot tube and hot wire probe

Figure 8 compares the calculated and experimental sound pressure spectrums for the 2-blade and 4-blade propeller fans. The sound pressure spectrums were evaluated by no frequency weighting characteristics, as it was called F-weighting, for comparison to calculated results. The sound pressure spectrums in Figure 8 were also normalized by subtracting the experimental overall aerodynamic noise level of the 4-blade propeller fan. Figure 8 shows frequency up to 1,240Hz as maximum. This was because Curle's equation used in the present study was assumed that sound source was compact. The maximum frequency 1,240Hz was calculated as sound wavelength with the equivalent size between hub to tip of blade. The calculated sound pressures were overestimated against the experimental results

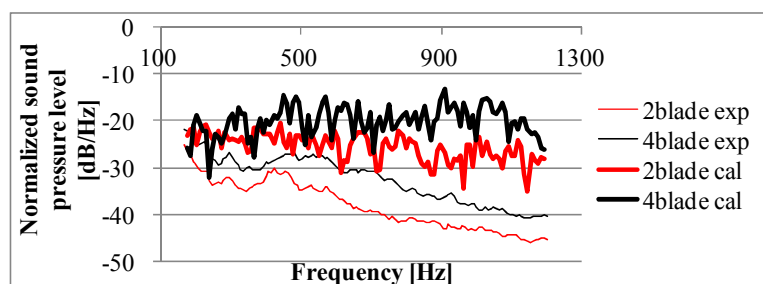


Figure 8: Comparison of sound pressure spectrums

Table 3 compares differences in overall value of the aerodynamic noise (OA) between the 2-blade and the 4-blade propeller fans, and also compares between calculated and experimental results. The calculated overall value was overestimated against the experimental one. However, the differences in overall value due to influence of blade number reasonably agreed. Aerodynamic noise was related to static pressure fluctuations according to Curle's equation. The static pressure fluctuations around blade and casing surfaces were attributed to velocity fluctuations around them. The overestimated calculated results in Figure 8 and Table 3 are therefore caused by the calculated velocity fluctuations in Figure 7.

Table 3: Differences in overall value of aerodynamic noise (OA)

-	2-blade	4-blade	-	exp.	cal.
exp. vs cal.	+10.5dB	+11.1dB	2-blade vs 4-blade	+5.7dB	+5.1dB

Consequently, we confirmed that the fan performance and the time-averaged velocity distributions reasonably agreed with the experimental results, and the tendencies of velocity fluctuations and sound pressure spectrums could be captured qualitatively, although more efforts for improvement of calculation quality still needed work. We therefore estimated that the calculated results captured main flow field structures, which played dominant roles with aerodynamic noise. Thus, the influence of blade number on aerodynamic noise was investigated by analyzing the calculated results, which was discussed in the next section.

Flow Structures

Figure 9 shows the flow structures colored with normalized helicity and limiting streamlines on the blade surface in a time-averaged flow field. The tip vortex (TV) of the 2-blade propeller fan rolled up from the tip near the leading edge. Streamlines are displayed around one of the TVs. The normalized helicity, H_n , of the TV maintained almost $H_n = +1.0$, and the TV passed through the blade-to-blade passage. Kusano et al. [9] also reported the same flow structure by calculating another half-ducted propeller fan. 3-blade propeller fan was intended and DES (Detached Eddy Simulation) was applied as numerical simulation method in their study.

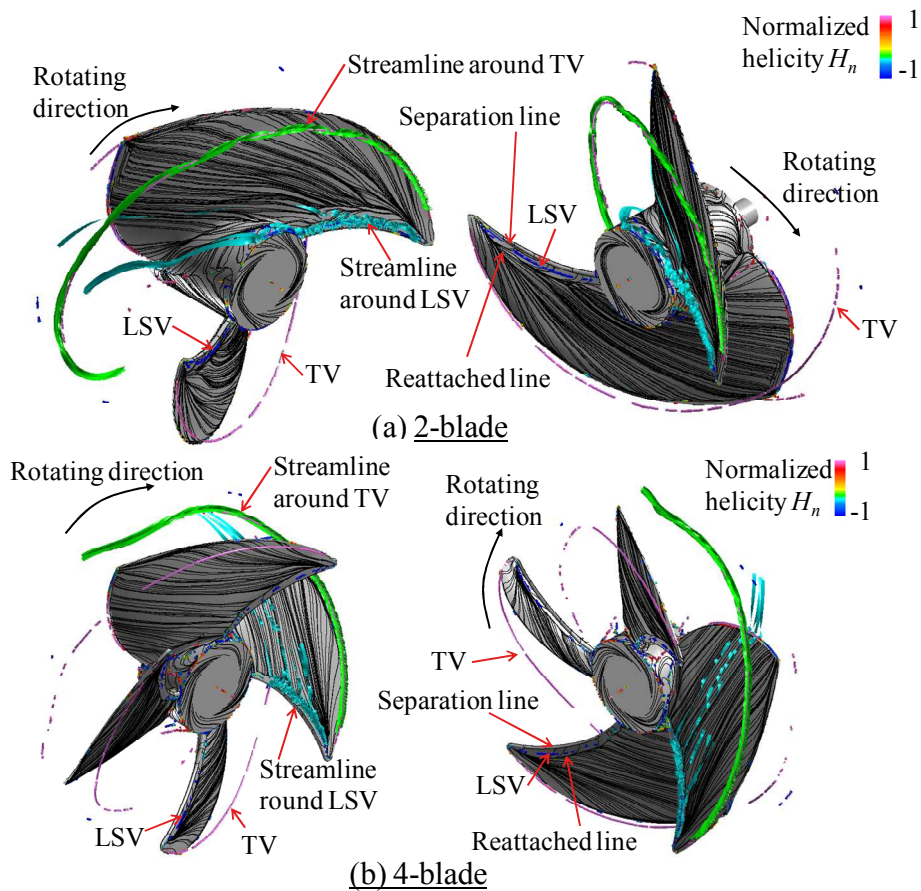


Figure 9: Vortex flow structures colored with normalized helicity and limiting streamlines on blade surface in time-averaged flow field

A separation line and reattached line in limiting streamlines could be found on the suction surface near the leading edge. Moreover, a vortex core was found near the leading edge between the separation line and the reattached line. The normalized helicity of this vortex core was $H_n = -1.0$.

This vortex could be a leading edge separation vortex (LSV) according to these results. The flow structures for the 4-blade propeller fan had the same tendency as the 2-blade propeller fan.

Therefore, we confirmed that TV and LSV had a great influence of flow structure on the 2-blade and 4-blade propeller fans. Thus, the influence of blade number on aerodynamic noise was investigated by taking particular note of TV and LSV.

Influence of blade Number on Aerodynamic Noise in LSV

Figure 10 shows turbulence intensity near LSV. Figure 11 shows the static pressure fluctuations on the suction surface. The static pressure fluctuation ΔC_p was normalized by density and propeller tip speed u_t . The turbulence intensities and the static pressure fluctuations near the LSV of the 2-blade and the 4-blade propeller fans were strong. The LSV increased the turbulence intensity and static pressure fluctuations. The turbulence intensity for the 2-blade propeller fan was stronger than that for the 4-blade propeller fan. However, the static pressure fluctuations for the 2-blade propeller fan were almost the same as those for the 4-blade propeller fan.

Aerodynamic noise was related to static pressure fluctuations according to Curle's equation, and the LSV therefore had a great influence on aerodynamic noise. However, we could not find any differences between the 2-blade and the 4-blade propeller fans in terms of LSV, because there were no differences of static pressure fluctuations between them.

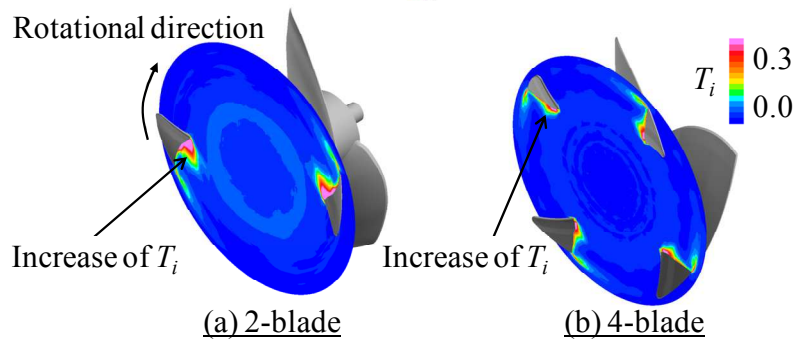


Figure 10: Turbulence intensity near LSV

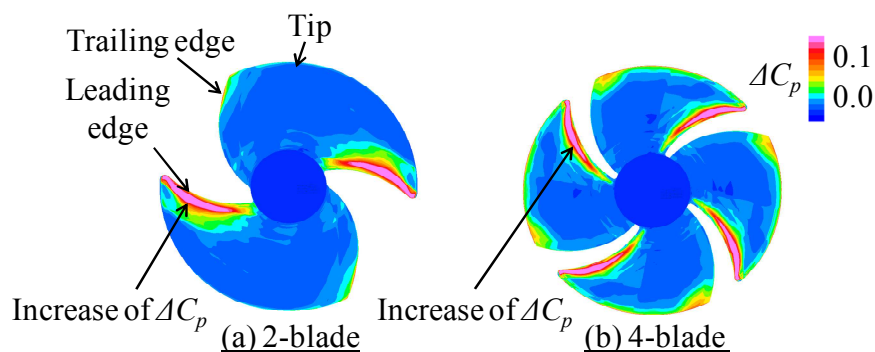


Figure 11: Static pressure fluctuations on suction surface

Influence of blade Number on Aerodynamic Noise in TV

Figure 12 shows vorticity and turbulence intensity near TV. The sections from A to H are perpendicular to TV. The vorticity is component ξ_a perpendicular to sections A-H. The vorticity decreased from section A to H. The turbulence intensity was strong near TV, on the other hand, especially in sections F, G, and H near the region where TV got closer to the ring. Figure 13 shows the relationship between the streamlines around the TV, ring, and adjacent blade. When TV reached the ring, it turned in a nearly tangential direction due to interaction between TV and the ring. Figure

14 shows static pressure fluctuations on the inner surface of the casing. The static pressure fluctuations of the 4-blade propeller fan were stronger than those of the 2-blade propeller fan. Figure 15 shows static pressure fluctuations on the pressure surface. The static pressure fluctuations near the trailing edge in the tip region of the 4-blade propeller fan were stronger than those of the 2-blade propeller fan.

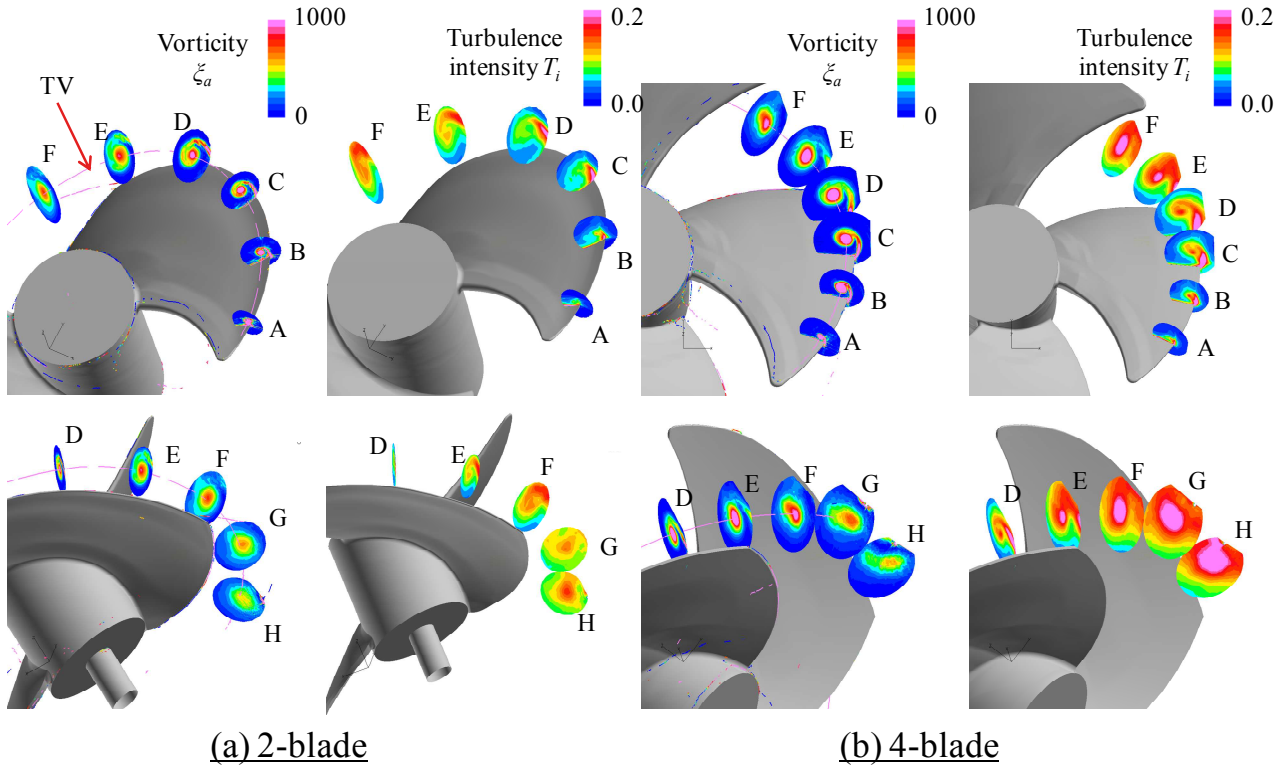


Figure 12: Vorticity and turbulence intensity near TV

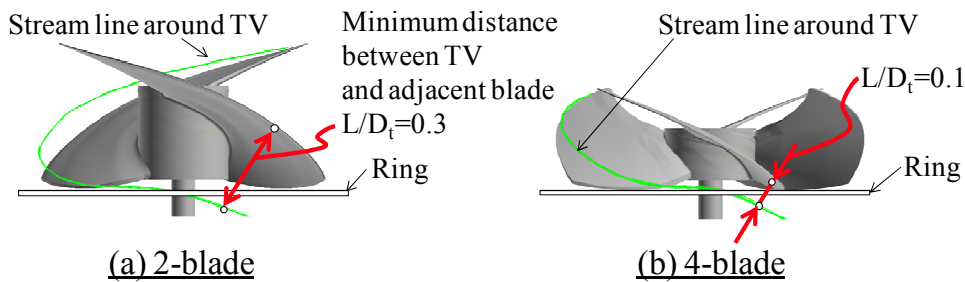


Figure 13: Relationship between streamline around TV, ring, and adjacent blade

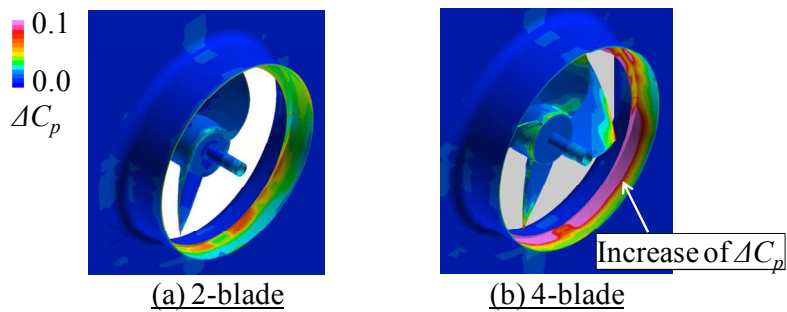


Figure 14: Static pressure fluctuations on inner surface of casing

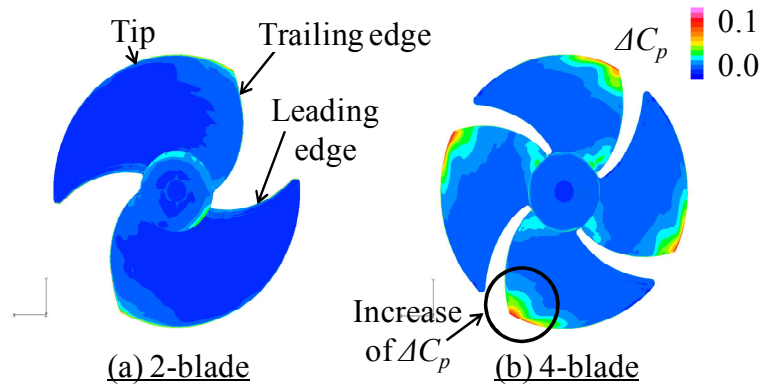


Figure 15: Static pressure fluctuations on pressure surface

The TV trajectory for the 2-blade propeller fan was longer than those for the 4-blade propeller fan shown in Figure 13. The vorticity of the 2-blade propeller fan therefore decayed along with TV than that of the 4-blade propeller fan. The TV of the 4-blade propeller fan reached the ring under the strong vorticity conditions shown in Figure 12. The increase of the turbulence intensity in sections F, G, and H caused strong interaction between TV and the ring in the 4-blade propeller fan shown in Figures 12 and 13. The increase of the turbulence intensity affects the strong static pressure fluctuations on the inner surface of the casing in the 4-blade propeller fan shown in Figure 14.

Moreover, the blade pitch of the 2-blade propeller fan is longer than that of the 4-blade propeller fan. The minimum distance between the streamline and the adjacent blade of the 2-blade propeller fan was three times longer than that of the 4-blade propeller fan shown in Figure 13. The interaction between TV and the adjacent blade was therefore strong in the 4-blade propeller fan because there was TV near the adjacent blade and vorticity was strong. As a result, the static pressure fluctuations on the pressure surface near the trailing edge at the tip region of the 4-blade propeller fan increased, as shown in Figure 15. Furthermore, the static pressure fluctuation on the suction surface near the trailing edge at the tip region of the 4-blade propeller fan also increased as shown in Figure 11. Therefore, the strong interaction between TV and the adjacent blade in the 4-blade propeller fan caused an increase in static pressure fluctuations on the pressure and the suction surfaces.

Aerodynamic noise was related to static pressure fluctuations according to Curle's equation, and TV therefore had a great influence on aerodynamic noise. The TV trajectory and the blade pitch of the 2-blade propeller fan were longer than those of the 4-blade propeller fan. These suppressed the interaction between TV, the ring, and adjacent blade, because the vorticity of the 2-blade propeller fan decayed along with TV more than that of the 4-blade propeller fan, and the minimum distance between TV and the adjacent blade of the 2-blade propeller fan was three times longer than that of the 4-blade propeller fan. The 2-blade propeller fan was therefore more silent than the 4-blade propeller fan.

CONCLUSIONS

Flow fields in the half-ducted propeller fans for the outdoor units of air-conditioners were calculated with finite element method-based large eddy simulation (LES) with the aim of investigating what influence of blade number had on aerodynamic noise in this study. 2-blade and 4-blade propeller fans were studied. The aerodynamic noise level of the 2-blade propeller fan was smaller than that of the 4-blade by 5.1 dB experimentally at an operating flow coefficient of $\phi=0.28$. The three main results can be summarized as follows:

1. The tip vortex (TV) rolled up from the tip near the leading edge. The leading edge separation vortex (LSV) was captured near the leading edge. The TV and LSV had a great influence of flow structure on the half-ducted propeller fan.

2. The LSV increased the turbulence intensity and static pressure fluctuations. The LSV therefore had a great influence on aerodynamic noise. However, we could not be found any difference between the 2-blade and 4-blade propeller fans in terms of the LSV.
3. The TV also increased the turbulence intensity and static pressure fluctuations. The TV therefore had a great influence on aerodynamic noise. The TV trajectory and blade pitch of the 2-blade propeller fan were longer than those of the 4-blade propeller fan. These suppressed the interaction between the TV, the ring, and adjacent blade, because the vorticity of the 2-blade propeller fan decayed along with the TV than that of the 4-blade propeller fan, and the minimum distance between TV and the adjacent blade of the 2-blade propeller fan was three times longer than that of the 4-blade propeller fan. The 2-blade propeller fan was therefore more silent than the 4-blade propeller fan.

REFERENCES

- [1] N. Hakamaya, S. Funabashi, and Y. Takada – *A Model for Predicting Noise of Propeller Fans in Air Conditioners*. Transactions of the Japan Society of Mechanical Engineers, Series B, Vol.65, No.640, pp.4015-4020, **1999**
- [2] C. Kato, M. Kaiho, and A. Manabe – *An Overset Finite Element Large Eddy Simulation Method with Application to Turbomachinery and Aeroacoustics*. J. Appl. Mech., Vol. 70, pp.32-43, **2003**
- [3] Y. Yamade, C. Kato, H. Shimizu, and T. Nishioka – *Large Eddy Simulation and Acoustical Analysis for Prediction of Aeroacoustics Noise Radiated From an Axial-flow Fan*. FEDSM2006-98303, Proceedings of the ASME Fluids Engineering Conference, Miami, FL, USA, **2006**
- [4] H. Reese, T. Carolus, and C. Kato – *Numerical Prediction of the Aeroacoustic Sound Sources in a Low Pressure Axial Fan without Inflow Distortion*. Proceedings of Fan Noise 2007 Symposium, Lyon, **2007**
- [5] C. M. Jang, M. Furukawa, and M. Inoue – *Analysis of Vortical Flow Field in a Propeller Fan by LDV Measurements and LES Part 1: Three-Dimensional Vortical Flow Structures*. Transactions of the ASME, Journal of Fluids Engineering, Vol.123, No.4, pp.748-754, **2001**
- [6] M. G. Beiler, and T. H. Carolus – *Computation and Measurement of the Flow in Axial Flow Fans with Skewed Blades*. ASME Journal of Turbomachinery, Vol.121, pp.59-66, **1999**
- [7] H. Okamoto, A. Goto, and M. Furukawa – *Design of a Propeller Fan using 3-D Inverse Design Method and CFD for High Efficiency and Low Aerodynamic Noise*. Proceedings of the ASME 2009 Fluids Engineering Division Summer Meeting, FEDSM2009-78454, **2009**
- [8] T. Sugio – *2 Wings Mixed Flow Fan for the Outdoor Unit of a Room Air Conditioner*. Turbomachinery, Turbomachinery Society of Japan, Vol.31, No.9, pp.520-524, **2003**
- [9] K. Kusano, J. H. Jeong, K. Yamada, and M. Furukawa – *Detached Eddy Simulation of Unsteady Flow Field and Prediction of Aerodynamic Sound in a Half Ducted Propeller Fan*. AJK2011-22048, Proceedings of the ASME-JSME-KSME Joint Fluids Engineering Conference, Hamamatsu, Shizuoka, Japan, **2011**
- [10] N. Curle – *The Influence of Solid Boundaries upon Aerodynamic Sound*. Proceedings of the Royal Society of London Series A-Mathematical and Physical Sciences, Vol.231, No.1187, pp.505-514, **1955**